Tropical and Extratropical Responses of the North Atlantic Atmospheric Circulation to a Sustained Weakening of the MOC

DAVID J. BRAYSHAW AND TIM WOOLLINGS

Department of Meteorology, University of Reading, Reading, United Kingdom

MICHAEL VELLINGA

Met Office Hadley Centre, Exeter, Devon, United Kingdom

(Manuscript received 17 April 2008, in final form 21 October 2008)

ABSTRACT

The tropospheric response to a forced shutdown of the North Atlantic Ocean's meridional overturning circulation (MOC) is investigated in a coupled ocean–atmosphere GCM [the third climate configuration of the Met Office Unified Model (HadCM3)]. The strength of the boreal winter North Atlantic storm track is significantly increased and penetrates much farther into western Europe. The changes in the storm track are shown to be consistent with the changes in near-surface baroclinicity, which can be linked to changes in surface temperature gradients near regions of sea ice formation and in the open ocean. Changes in the SST of the tropical Atlantic are linked to a strengthening of the subtropical jet to the north, which, combined with the enhanced storm track, leads to a pronounced split in the jet structure over Europe. EOF analysis and stationary box indices methods are used to analyze changes to the North Atlantic Oscillation (NAO). There is no consistent signal of a change in the variability of the NAO, and while the changes in the mean flow project onto the positive NAO phase, they are significantly different from it. However, there is a clear eastward shift of the NAO pattern in the shutdown run, and this potentially has implications for ocean circulation and for the interpretation of proxy paleoclimate records.

1. Introduction

In recent years there has been considerable academic and popular interest in the possibility of a weakening or even a shutdown of the North Atlantic Ocean's meridional overturning circulation (MOC). Indeed, the fourth Intergovernmental Panel on Climate Change (IPCC) assessment report states that, based on the currently available simulations, it is very likely that the Atlantic MOC will weaken over the twenty-first century (Meehl et al. 2007), although the possibility of a complete shutdown over longer time scales remains a matter of considerable debate.

The impact of such a weakening will be communicated to the European continent primarily through changes in the atmosphere and, in particular, the North Atlantic storm track, which describes the aggregate path of the mobile synoptic-scale cyclonic systems that are responsible for much of the region's day-to-day weather. Large-scale circulation patterns, such as the North Atlantic Oscillation (NAO) are also to be affected.

This paper examines the wintertime [December–February (DJF)] atmosphere's response in the North Atlantic region to a forced shutdown of the Atlantic MOC in the third climate configuration of the Met Office Unified Model (HadCM3), adding detail to previous studies that do not directly analyze the storm-track and NAO responses. Overall, the MOC weakening is found to produce a stronger North Atlantic storm track, driving stronger westerly surface flow into Europe, but producing cooler surface temperatures and slightly reduced precipitation, consistent with a study by Jacob et al. (2005), who used a different climate model.

A brief description of the experimental configuration is provided in section 2; this is followed by a discussion of the changes in the North Atlantic storm track and the dynamical mechanisms causing them. ''Local'' forcings are discussed in section 3, while section 4 focuses on the impact of oceanic changes that occur in the tropical

Corresponding author address: David Brayshaw, P.O. Box 243, Department of Meteorology, University of Reading, Earley Gate, Reading, RG6 6BB, United Kingdom.
E-mail: d.j.brayshaw@reading.ac.uk

DOI: 10.1175/2008JCLI2594.1

Atlantic. Changes in the NAO pattern and its variability are discussed in section 5. Section 6 presents a summary discussion and the main conclusions.

2. Experiment outline

The experimental configuration is presented in detail in Vellinga and Wu (2008) and a brief description of the experiments is provided below.

The experiments use the HadCM3 coupled ocean–atmosphere GCM. This model has a resolution of 2.5° × 3.75° in the atmosphere and 1.25° × 1.25° in the ocean and has been extensively used for climate prediction and research. Fixed preindustrial values are used throughout this paper for the insolation parameters and the chemical composition of the atmosphere.

A control run simulation of HadCM3 performed under these conditions produces a stable North Atlantic MOC of around 20 Sv (1 Sv $\equiv 10^6$ m^3 s^{-1}). A shutdown of the MOC is then forced by adding a continuous freshwater flux (1.1 Sv) in the high-latitude North Atlantic. ''Hosing'' the ocean in this manner reduces its density at high latitudes and is a commonly used method to weaken the MOC in GCM simulations. This hosing is very strong and is not intended to be an accurate simulation of, for example, a realistic melting rate for the Greenland ice sheet. The hosing is applied continually throughout a 240-yr integration to maintain a forced ''MOC-off'' state. Only data from years 220 to 240 are used, when the model has reached a new quasi-equilibrium state (as indicated by a net radiative balance at the top of the atmosphere). Data from 20 yr of boreal winters (December–February) are collected from the hosed simulation and are compared to 20 yr of the control run.

The storm tracks are diagnosed by applying a 2–6-day bandpass Lanczos filter (Duchon 1979) to 6-hourly mean sea level pressure (MSLP) data to create variance maps. Similar results are, however, obtained if either alternative variance statistics (e.g., meridional heat transport at 850 hPa) or Lagrangian feature tracking of vorticity centers at 850 hPa (Hoskins and Hodges 2002) are used. The statistical significance of the storm-track changes are assessed using the Wilcoxon–Mann–Whitney test (Wilks 1995). The main changes in the storm track described in this paper are significant at well over the 90% level.

The general characteristics of the storm tracks produced by this model are discussed by Greeves et al. (2007), Ringer et al. (2006), Stratton (2004), and Pope and Stratton (2002) in the context of their sensitivity to spatial resolution and model development. Those authors find that the model produces a reasonable representation of the Northern Hemisphere storm tracks when compared to operational forecast models (Stratton 2004), although they tend to be rather weaker than and shifted slightly southward of those in the observations (e.g., Uppala et al. 2005), with the North Atlantic storm track also tending to weaken more rapidly downstream over Europe. Comparison between the storm track (as measured by the MSLP variance) in the ''preindustrial'' control run used in this paper and the 40-yr European Centre for Medium-Range Weather Forecasts (ECMWF) Re-Analysis (ERA-40; Uppala et al. 2005) indicates similar differences, but, overall, the model represents the expected large-scale features of the storm track reasonably well (cf. Figs. 1a,c).

Changes in the NAO are assessed using both a stationary ''box-averaged'' method and an EOF analysis. The details of this are described in section 5.

3. Storm-track changes

The changes in the North Atlantic storm tracks produced by the hosing are shown in Fig. 1. While both the hosed and control runs show the track extending from the Newfoundland, Canada, area into northwestern Europe, the track in the hosed simulation is much stronger than that in the control run and extends much farther into Europe (the MSLP variance is approximately doubled over Iceland, the United Kingdom, and Scandinavia). Over the upstream (western) side of the Atlantic there is evidence of intensification and a slight northward shift in the track (the peak MSLP variance is almost 50% stronger in the hosed run). In the Pacific, there is a similar but weaker increase in storm-track intensity measured by MSLP variance (not shown).

Because the storm tracks are responsible for much of the poleward heat transport in the midlatitudes, the changes in the poleward heat transport by the storm track (2–6-day bandpass-filtered $\overline{v'T'}$ at 850 hPa, not shown) are similar in structure to those seen in the MSLP variance over the North Atlantic (Fig. 1). Over the western Atlantic, the bandpass-filtered $\overline{v'T'}$ at 850 hPa is approximately doubled, with even stronger fractional increases downstream over northern Europe. Such changes are consistent with the atmosphere acting to partially compensate for the reduced northward heat transport by the ocean [Vellinga and Wu (2008) describe the changes in the zonal-mean energy transport in these simulations].

The results of the cyclone-tracking analysis are in good agreement with the changes seen in Fig. 1, so they are not shown here. In the tracking analysis the general strength of the storm track is represented by the track

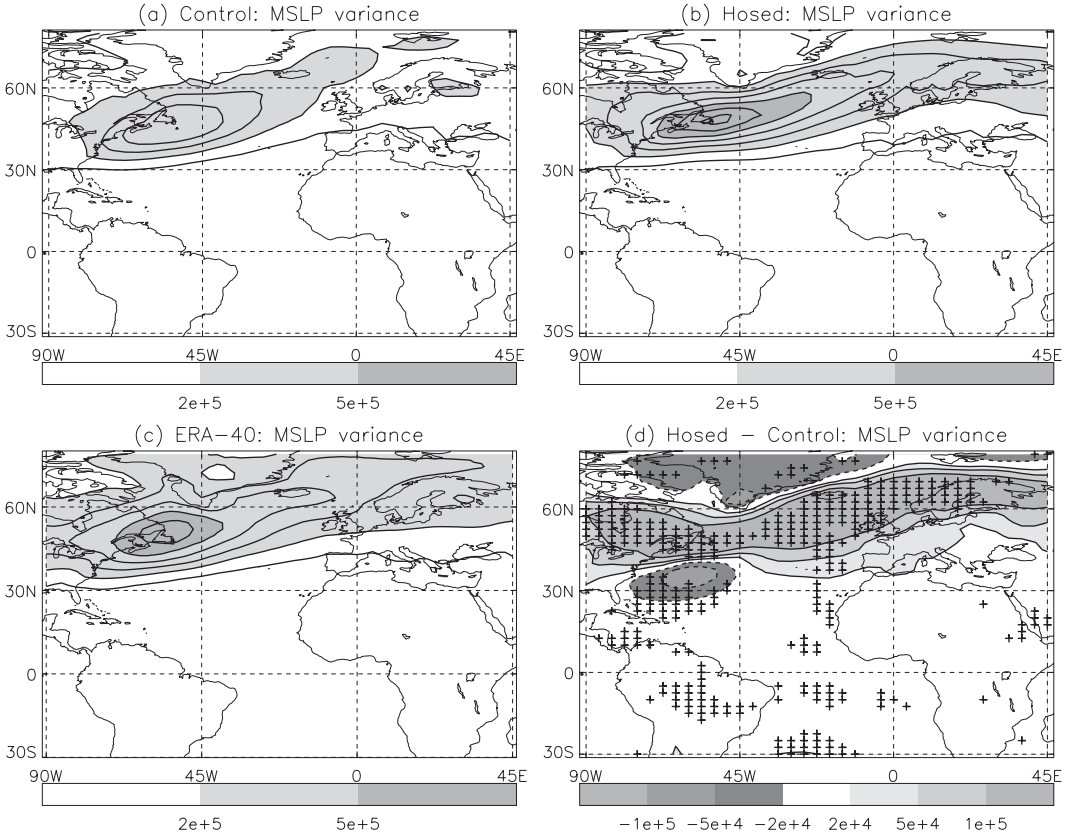

FIG. 1. The storm tracks (variance of 2–6-day bandpass-filtered MSLP). (a) The control run, (b) the hosed run, and (c) ERA-40 (winters only from 1978/79 to 2001/02), with contours every 10^5 Pa^2. (d) The difference (hosed − control), with negative changes indicated by dashed contours. Areas where the change is significant at the 99% level are marked with "+" symbols. All data are for DJF.

density, defined as the average number of cyclones per winter per unit area, where one unit area corresponds to a 5° spherical cap. The changes in track density mirror those in Fig. 1d, showing that the increase in variance is associated with higher storm counts. In contrast, the tracking shows no significant change in the mean intensity or lifetime of cyclone tracks in this region. However, it should be noted that, when compared to observations, the individual storms in the model tend to be too weak and too long lived, and have slower growth and decay rates (Stratton 2004; Greeves et al. 2007). It is therefore possible that this result could be affected by these model deficiencies.

The pattern of change in the North Atlantic storm track is consistent with the changes in the surface temperatures of the region. Comparing Fig. 2b with Fig. 2a shows that the hosing leads to cooler sea surface temperatures (SSTs) in the North Atlantic (the difference is shown in Fig. 2c) and a marked increase in the sea ice extent in the northern oceans. This leads to a tightening of the surface temperature gradients throughout most of the North Atlantic, but particularly in the region of Newfoundland (near the southern edge of the sea ice in Fig. 2b) and in the open ocean to the west of Portugal, Spain, and the United Kingdom. The increases in the surface temperature gradient are consistent with increases of the near-surface baroclinicity (measured by the Eady growth rate) in these regions as shown in Fig. 2d, which leads to the changes in the storm track shown in Fig. 1. In agreement with this, the tracking analysis shows that cyclogenesis in the Newfoundland region is increased by around 40% (measured in average number of genesis events per winter per unit area).

Despite the increase in strength of the storm track in the hosed experiment, the precipitation over the North Atlantic and European area is slightly reduced (Fig. 3). This is consistent in sign with the reduction in surface temperature throughout the sector, which reduces the saturation water vapor pressure of the air as expected from the Clausius–Clapeyron relationship. The surface climate of Europe is therefore cooler and drier, despite the storm track driving a stronger westerly maritime flow, in agreement with the results presented by Jacob et al. (2005).

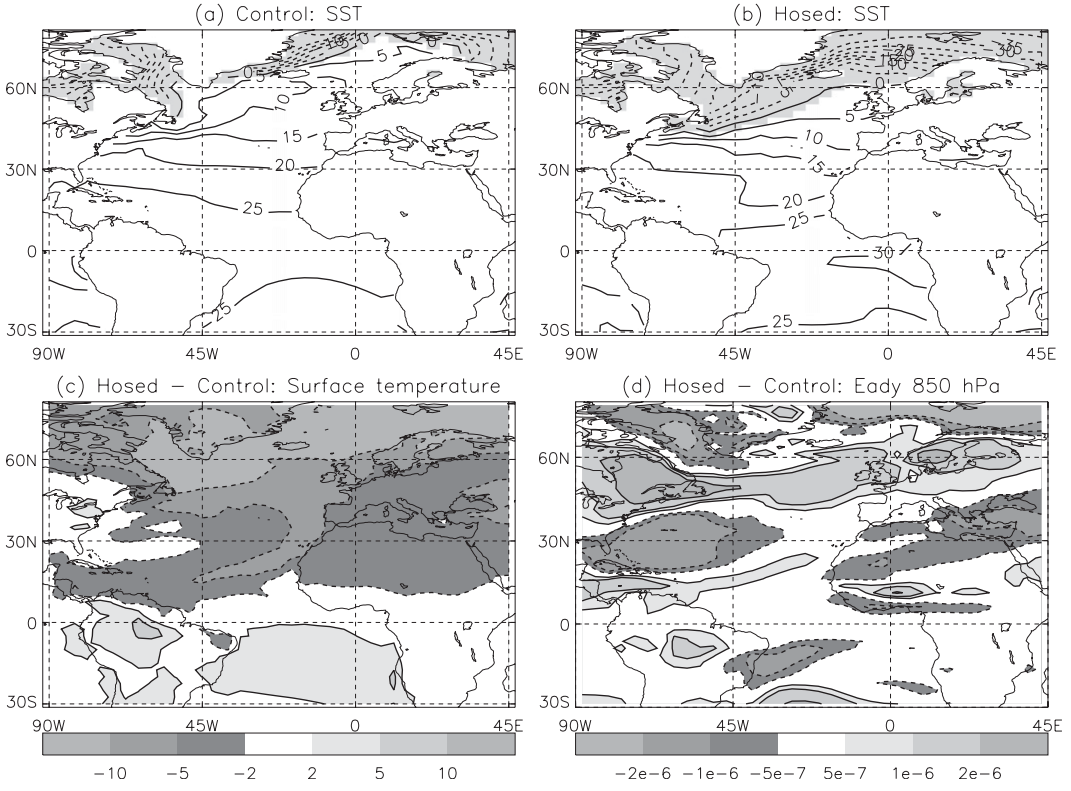

FIG. 2. Surface properties. (a),(b) Sea surface temperature (contours at 5°C, dashed for negative) and area of sea ice cover (shaded where sea ice fraction in a grid box exceeds 4%) for the control and hosed experiments, respectively; (c) the change in surface temperature (hosed − control, including changes over land areas); and (d) the Eady growth rate anomaly (hosed − control) at 850 hPa (s^{-1}). All data are for DJF and negative values are indicated by dashed contours.

4. Tropical and subtropical changes

In addition to providing a "local" forcing of the storm track through changes in the North Atlantic surface temperatures, the freshwater hosing also modifies the climate in remote regions. Examining Fig. 2c shows that while the North Atlantic SST is cooled by the hosing, parts of the tropical and southern Atlantic are warmed. This is consistent with the 5°–10° southward shift and intensification of the tropical precipitation over the ocean in the hosed experiment (Fig. 3). The changes in diabatic heating over the tropics are discussed in more detail by Vellinga et al. (2002).

In the time mean, the latent heat released by the precipitation is balanced by adiabatic cooling and ascent, leading to convergent horizontal flow in the lower troposphere and divergent horizontal flow in the upper troposphere (through conservation of mass). Following Sardeshmukh and Hoskins (1988), and ignoring vortex twisting terms, it is possible to write the vorticity equation as

$$\frac{\delta\zeta}{\delta t} + \mathbf{v}_\psi \cdot \nabla\zeta = -\zeta\nabla\cdot\mathbf{v}_\chi - \mathbf{v}_\chi\cdot\nabla\zeta + F, \qquad (1)$$

where ζ is the absolute vorticity, $\mathbf{v}_\psi$ and $\mathbf{v}_\chi$ are the horizontal velocity fields associated with rotational and divergent flow, respectively, and F is the frictional term. Considering the time mean and decomposing the divergence terms into their mean and transient parts then gives

$$\overline{\mathbf{v}_\psi\cdot\nabla\zeta} = -\bar{\zeta}\nabla\cdot\bar{\mathbf{v}}_\chi - \bar{v}_\chi\beta - \bar{\mathbf{v}}_\chi\cdot\nabla\bar{\xi} - \overline{\zeta'\nabla\cdot\mathbf{v}'_\chi} - \overline{\mathbf{v}'_\chi\cdot\nabla\zeta'} + \bar{F}, \qquad (2)$$

where ξ is the relative vorticity, while bars and primes indicate time means and anomalies, respectively.

The terms on the right-hand side of Eq. (2) can therefore be considered as a vorticity source that is balanced (in the time mean) by the advection of vorticity by the rotational flow. The structure of the first two terms for both the upper and lower troposphere is shown in Fig. 4 (the magnitude of the third term, $|\bar{\mathbf{v}}_\chi\cdot\nabla\bar{\xi}|$, is rather small in practice). From these figures it is therefore possible to assess the vorticity tendency that would be associated with each of the terms and to consider the rotational flow that would be consistent with balancing

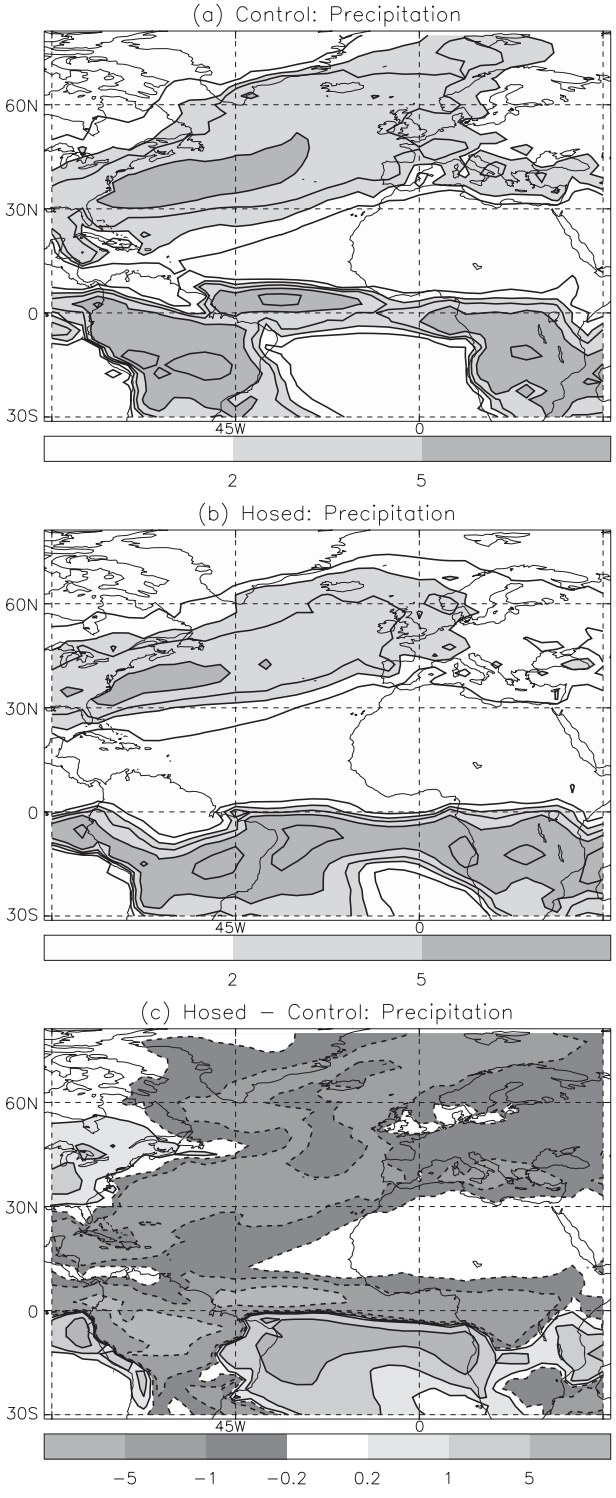

FIG. 3. Precipitation (mm day^{-1}) in (a) the control run and (b) the hosed run; contours at 1, 2, 3, 5, and 10 mm day^{-1}. (c) The difference (hosed − control), with negative changes indicated by dashed contours. All data are for DJF.

that forcing if all the other terms were assumed to be negligible (unfortunately data are not available to assess the transient terms). These assessments can then be compared against the observed rotational flow as indicated by the time-mean streamfunction.[1]

Consider first the upper troposphere. Figure 4a shows that the region of increased precipitation (a band running from 35°W to 10°E at 10°–15°S) is collocated with upper-tropospheric divergence and the generation of a positive vorticity tendency (i.e., anticyclonic flow in the Southern Hemisphere). This is consistent with the anticyclonic anomaly to the south (the streamfunction minimum centered at 20°S, 30°W), which acts to balance this by the northward advection of high negative vorticity air on its eastern side (i.e., $\bar{v}_\psi\beta$ is positive there). The vorticity forcing associated with the convergence anomaly above the region of decreased precipitation to the north (0°–5°N, 50°–20°W) is rather weak because $|f|$ and, consequently, $|\bar{\zeta}\nabla\cdot\bar{\mathbf{v}}_\chi|$ are small near the equator.

The second term $-\bar{v}_\chi\beta$ is large and negative over the equator to the north of the divergence region (centered on 0°N, 25°W in Fig. 4b) and is due to enhanced northward divergent flow across the equator in the upper troposphere. The anticyclonic rotational flow anomaly (negative vorticity anomaly) centered on 15°N, 10°W is consistent with balancing this forcing resulting from the southward advection of high-vorticity air on its eastern side (i.e., $\bar{v}_\psi\beta$ is negative there). This anticyclone is then consistent with the enhancement of the subtropical jet in the Northern Hemisphere in the region around 20°–30°N, 30°–10°W (Fig. 5). This analysis therefore suggests that changes in the tropical SST structure in the Southern Hemisphere are impacting the subtropical jet structure of the Northern Hemisphere and are capable of acting as a source of Rossby waves in the Northern Hemisphere (as in Sardeshmukh and Hoskins 1988), although such waves are not examined in detail here.

In the lower troposphere, Fig. 4c shows that the anomalous convergence associated with the increased precipitation acts as a source of negative vorticity. This is therefore consistent with the cyclonic streamfunction anomaly to the south (centered on 25°S, 30°W), which again acts to balance this tendency. The origin of the

[1] It should be noted that the left-hand side of Eq. (2) also contains transient components (i.e., $\mathbf{v}_\psi\cdot\nabla\zeta = \overline{\mathbf{v}'_\psi\cdot\nabla\zeta'} + \bar{v}_\psi\cdot\nabla\bar{\zeta}$) that cannot be accounted for by examining the time-mean streamfunction. The term $\overline{\mathbf{v}'_\psi\cdot\nabla\zeta'}$, and the transient terms on the right-hand side of Eq. (2), may modify the details of the tropical response. However, despite this limitation, analysis of the time-mean components still provides useful insight into the tropical forcing and the circulation response that it supports.

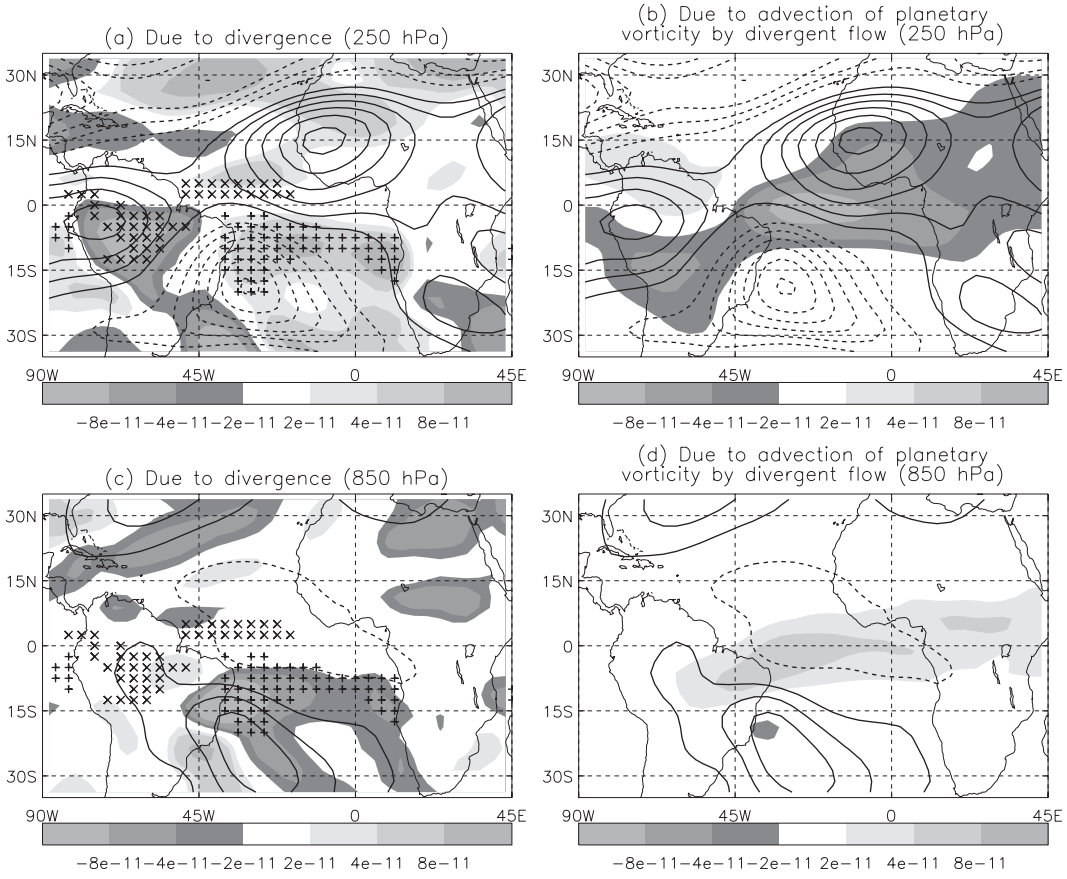

FIG. 4. The tropical response to the hosing. The shading in (a) and (b) shows the anomaly (hosed − control; s^{-2}) in first two terms in Eq. (2) calculated at 250 hPa: (a) $-\bar{\zeta}\nabla\cdot\bar{\mathbf{v}}_\chi$ and (b) $-\bar{v}_\chi\beta$. Positive values can be interpreted as a positive vorticity tendency that must be balanced by the rotational flow (see text). Contours indicate streamfunction anomalies at 250 hPa (contours every 2×10^6 m^2 s^{-1}, with negative values indicated by dashed contours). The + and × symbols in (a) indicate regions where precipitation is increased/reduced by more than 5 mm day^{-1}. (c),(d) Same as (a),(b), but for the 850-hPa level. All data are for DJF.

signal in the rotational flow to the north is less clear, but is, however, consistent with similar arguments. The rotational flow anomalies in the lower troposphere therefore lead to a westerly flow anomaly over tropical South America (as indicated by the streamfunction values in Fig. 4c), weakening the trade easterly winds and reducing the supply of moisture and precipitation to the continental interior (approximately 5°S, 60°W in Fig. 3).

Examination of Figs. 4b,d also suggests that the response to the tropical SST anomalies could alternatively be considered as a zonally localized enhancement of the Hadley cell (cf. Zhang and Delworth 2005) and, consequently, the subtropical jet (these figures show $-\bar{v}_\chi\beta$; therefore, the negative values in Fig. 4b indicate a northward flow at upper levels, whereas the positive values in Fig. 4d indicate a southward flow at lower levels). This enhancement of the subtropical jet in the North Atlantic (and indeed downstream into northern Africa and Eurasia) is associated with increased baroclinicity along its northern flank in the upper troposphere (not shown). However, while the increase in baroclinicity is consistent in sign with the changes in the storm track, it lies far to the south (the northern flank of the subtropical jet lies at around 20°–30°N, whereas the storm track occurs at 45°–50°N; cf. Fig. 1 with Fig. 5). This leads to a clear split between the eddy-driven and subtropical jets in the upper troposphere over Europe in the hosed simulation (Fig. 5b) and a stronger subtropical jet downstream toward India.

5. NAO

The NAO is the dominant pattern of atmospheric variability over the Atlantic, and is of particular interest here given that changes in the NAO can potentially feed back onto the MOC (e.g., Marshall et al. 2001). This section investigates whether the nature of NAO variability is affected by a shutdown of the MOC.

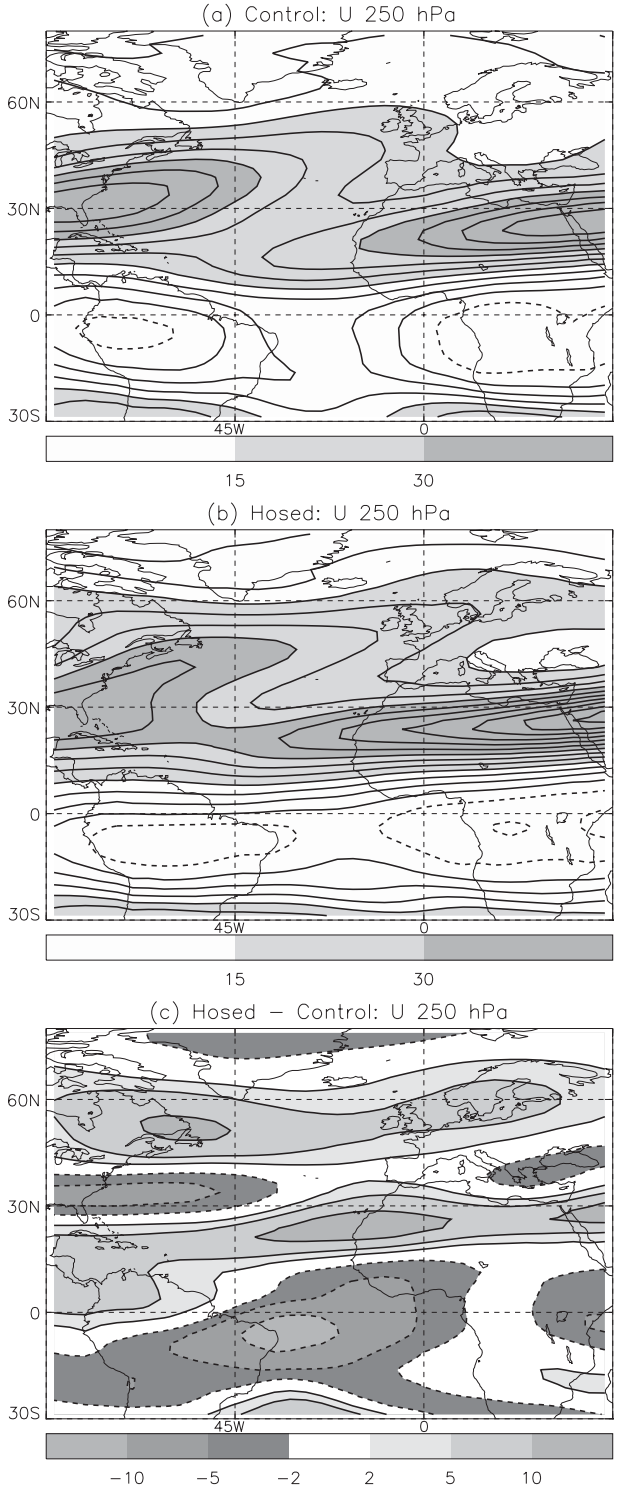

FIG. 5. Zonal wind at 250 hPa in (a) the control run and (b) the hosed run; contours at −10, 0, 10, 15, 20, 25, 30, 40, 50, and 60 m s^{-1}. (c) The difference (hosed − control). All data are for DJF and negative values are indicated by dashed contours.

In each experiment, the NAO is identified as the first empirical orthogonal function (EOF) of DJF monthly MSLP anomalies over the Northern Hemisphere sector of 120°W–90°E. The resulting patterns are shown in Fig. 6 by regressing the MSLP onto the principal component time series. Both patterns account for similar amounts of variance (32% and 35%, respectively), and the patterns are not sensitive to changes in the region used for the analysis (e.g., over the Atlantic/European region the leading EOFs of hemispheric MSLP are very similar to those shown). The hosing run shows a clear eastward shift of the NAO pattern and a downstream extension of the northern center. The pattern shifts to the extent that in the hosed experiment Iceland experiences the temperature variations associated with the NAO, while in the control run Iceland sits on the middle of the temperature ''seesaw'' between Greenland and Scandinavia (as seen in observations). This is seen by regressing lower-tropospheric temperature on the principal component time series, as shown in Fig. 7. These changes in the NAO pattern are consistent with the storm-track extension described previously, because the NAO is closely linked to variations in the orientation of the North Atlantic storm track. If the storm track extends farther downstream, then so will the signature of its variations.

The fact that the NAO pattern has changed may have implications for the interpretation of paleoclimate records. When using proxy data at a given location to infer climate data, it may be important if variations in the NAO have affected that location differently during different periods. The change in pattern may also have an effect on the ocean, as follows. Over the Labrador Sea the pressure gradient associated with the NAO pattern is much weaker in the hosing run. Variability of the NAO therefore has a weaker influence on surface winds there than it does in the control run, and thus a potentially weaker influence on Labrador Sea deep convection (Dickson et al. 1996). In the model runs this is not particularly relevant, because in the hosing run there is no deep convection in any case. The relevance to the real world presumably depends on the extent to which the pattern changes if the MOC is just weakened rather than shut down.

Following Stephenson et al. (2006), a stationary NAO index is defined as the difference in absolute MSLP averaged over the southern (20°–55°N, 90°W–60°E) and northern (55°–90°N, 90°W–60°E) halves of the Atlantic sector. This index can be interpreted as an absolute measure of the strength of zonal flow, and its daily distribution is shown in Fig. 8a for both runs. There is an increase in the mean value of this index, from 1.4 hPa in the control run to 4.3 hPa in the hosing run, consistent with the enhanced storm track driving stronger westerly

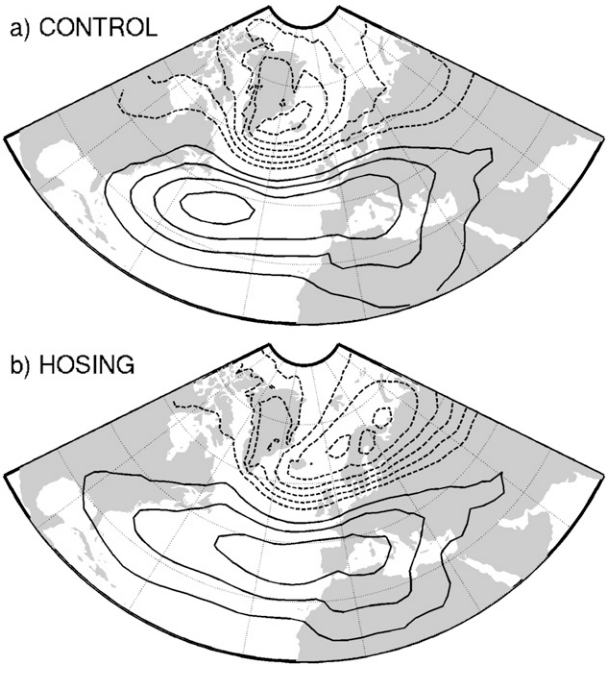

FIG. 6. First EOF of DJF monthly mean MSLP over the Atlantic sector from the (a) control and (b) hosing runs. Contours are drawn every 1 hPa per standard deviation of the principal component time series, with negative contours dashed and the zero contour omitted.

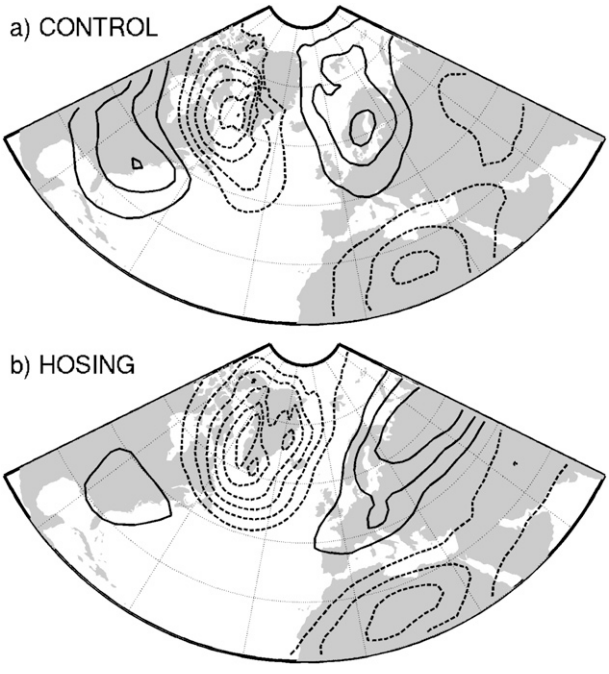

FIG. 7. Temperature at 850 hPa regressed onto the principal components of the MSLP EOFs in Fig. 6. Contours are drawn every 0.5 K per standard deviation of the time series, with negative contours dashed and the zero contour omitted.

flow across the Atlantic. The mean surface pressure change is very similar to that shown in Vellinga and Wood (2002) and, while this projects onto the stationary NAO index, the pattern is significantly different from that of the NAO. This increase in surface westerlies over the Atlantic potentially has consequences for the gyre circulation in the ocean (Marshall et al. 2001). There is no significant change in the variance of this index between the two runs, so that the magnitude of variations in the NAO is unchanged.

In Fig. 8a there appears to be a change in the skewness of the NAO index, suggesting a change in the nature of NAO variability so that the positive phase is realized more often. If the data are sampled every 10 days to account for autocorrelation, then the distributions are only just significantly different from normal at the 90% level using a Lilliefors test. However, a different daily NAO index, calculated by projecting the daily MSLP anomalies onto the pattern of the first EOF (Fig. 8b), does not suggest any change in the nature of variability, and in both runs this index is normally distributed. This difference arises because there is an asymmetry between the positive and negative phases of the NAO, and it is especially clear for the hosing run, where extreme positive NAO days have a weaker projection onto the box index than extreme negative days. This occurs because the southern center is weaker and the northern center more confined in the positive phase when compared with the negative phase.

There is therefore no consistent signal of a change in the variance or distribution of the NAO, although the presence of stronger westerlies in the time mean is clear. However, the changes in the NAO pattern described above also emerge as a robust feature of several other methods of analysis, for example, a regression of MSLP or 850-hPa temperature onto the stationary box index, and also a teleconnectivity analysis of MSLP (not shown).

6. Discussion and conclusions

This note has discussed the changes in the winter (DJF) North Atlantic storm track, the subtropical jet, and the NAO produced by an artificially induced shutdown of the MOC in a freshwater hosing experiment, as described in Vellinga and Wu (2008). The prolonged MOC shutdown and the associated changes in the North Atlantic SST are found to greatly increase the strength of the storm track throughout the North Atlantic sector and (more weakly) throughout the whole of the northern midlatitudes. The North Atlantic storm track shifts slightly northward near the east coast of North America and penetrates more deeply into western Europe. Despite the increased westerly flow bringing more maritime air

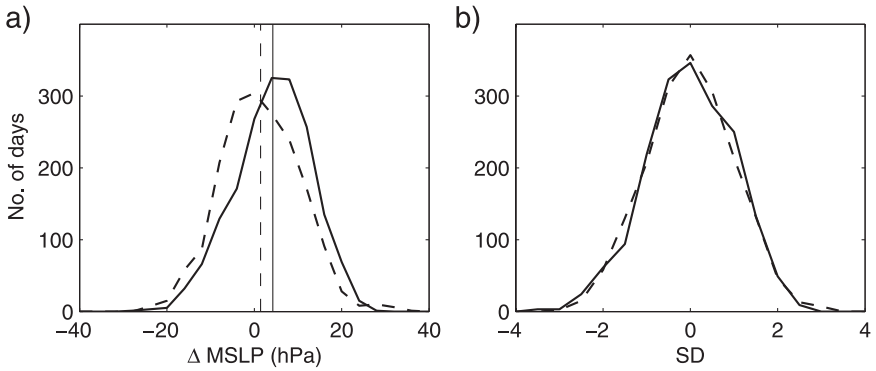

FIG. 8. (a) Distribution of the daily-mean MSLP difference: southern box − northern box. Vertical lines mark the means. (b) Distributions (std dev) of the NAO index obtained by an area-weighted projection of daily MSLP anomalies onto the leading EOF patterns. The dashed lines are for the control run and the solid lines are for the hosing run.

into Europe, surface temperatures and precipitation are reduced consistent with the cooler upstream ocean (as seen in previous studies).

The increases in storm activity are closely related to changes in the near-surface baroclinicity in the region. These changes are consistent with the increased SST gradients in the mid-Atlantic and the tight surface temperature gradients produced near the southern edge of the sea ice that forms off the coast of Newfoundland in the hosed simulation.

The MOC shutdown also leads to a southward shift of the ITCZ in the tropical Atlantic and complex patterns of change in precipitation over tropical South America. This drives an enhanced subtropical jet over the tropical North Atlantic, which, when combined with the increase in the storm-track strength farther to the north, leads to a clear split in the upper-tropospheric jet over Europe. The enhancement in the subtropical jet also continues well downstream of the Atlantic sector toward India.

Previous studies (Brayshaw et al. 2008; Nakamura et al. 2004) have indicated that the relative latitudinal positions and intensities of the midlatitude surface temperature front (MSTF) and the subtropical jet (STJ) are closely linked to the strength of the storm track and the position of the eddy-driven jet. In particular, when starting from a position where the MSTF and STJ are well separated, the storm track tends to become stronger as they are brought closer together (see Table 2 in Brayshaw et al. 2008). It is therefore interesting to note that the relationship between the MSTF and the STJ in the North Atlantic sector has changed in the hosed simulation relative to that in the control run, and that the separation between them has slightly increased [Figs. 2a,b show that the MSTF has intensified and perhaps shifted slightly northward over the upstream part of the Atlantic (also seen in the change in the near surface baroclinicity in Fig. 2d), while the STJ is enhanced over the North Atlantic Ocean but perhaps shifted slightly southward over the Sargasso Sea; see Fig. 5c]. This suggests that the increase in the intensity of the storm track in the North Atlantic sector of the hosed simulation could be even stronger if the MSTF–STJ separation was reduced (i.e., the storm track might have been stronger if the MSTF–STJ separation had remained the same as it was in the control simulation). Further experiments would, however, be required to investigate this possibility and its impact on the poleward energy transport by the atmosphere (Vellinga and Wu 2008).

The pattern of changes in the mean flow projects onto the positive NAO state (whether defined by box-averaged or EOF techniques). However, the pattern of mean flow change is significantly different from that of the NAO, and there is no significant change in the occupancy of the positive and negative states of the NAO. There is a clear eastward shift of the NAO pattern in the hosed simulation, and this has several implications. It has an important effect on the nature of the variability seen at various locations. For example, the influence of the NAO on surface pressure over Scandinavia is doubled, and both Iceland and northern Russia experience temperature variations associated with the NAO, while they did not in the control run. The pattern change may have implications for the interpretation of proxy records for climate data, which assume that patterns of variability are unchanged even in quite different climates. Finally, the changes in both the mean flow and the NAO pattern may potentially feed back onto the ocean circulation.

Acknowledgments. The authors thank Prof. Brian Hoskins for his helpful comments and the two anonymous reviewers whose comments have also helped to improve this note.

DJB and TW were supported by the NERC Rapid Climate Change Program, under projects NER/T/S/2002/00441 and NE/C509115/1, respectively. MV was supported by the Defra and MoD Integrated Climate Programme (GA01101, CBC/2B/0417Annex C5).

REFERENCES

Brayshaw, D. J., B. Hoskins, and M. Blackburn, 2008: The storm track response to idealized SST perturbations in an aquaplanet GCM. *J. Atmos. Sci.,* **65,** 2842–2860.

Dickson, R., J. Lazier, J. Meincke, P. Rhines, and J. Swift, 1996: Long-term coordinated changes in the convective activity of the North Atlantic. *Prog. Oceanogr.,* **38,** 241–295.

Duchon, C. E., 1979: Lanczos filtering in one and two dimensions. *J. Appl. Meteor.,* **18,** 1016–1022.

Greeves, C. Z., V. D. Pope, R. A. Stratton, and G. M. Martin, 2007: Representation of Northern Hemisphere winter storm tracks in climate models. *Climate Dyn.,* **28,** 683–702.

Hoskins, B. J., and K. I. Hodges, 2002: New perspectives on the Northern Hemisphere winter storm tracks. *J. Atmos. Sci.,* **59,** 1041–1061.

Jacob, D., H. Goettel, J. Jungclaus, M. Muskulus, R. Podzun, and J. Marotzke, 2005: Slowdown of the thermohaline circulation causes enhanced maritime climate influence and snow cover over Europe. *Geophys. Res. Lett.,* **32,** L21711, doi:10.1029/2005GL023286.

Marshall, J., H. Johnson, and J. Goodman, 2001: A study of the interaction of the North Atlantic Oscillation with ocean circulation. *J. Climate,* **14,** 1399–1421.

Meehl, G. A., 2007: Global climate projections. *Climate Change 2007: The Physical Science Basis,* S. Solomon et al., Eds., Cambridge University Press, 747–847.

Nakamura, H., T. Sampe, Y. Tanimoto, and A. Shimpo, 2004: Observed associations among storm tracks, jet streams, and midlatitude oceanic fronts. *Earth's Climate: The Ocean-Atmosphere Interaction, Geophys. Monogr.,* No. 147, Amer. Geophys. Union, 329–345.

Pope, V. D., and R. A. Stratton, 2002: The processes governing horizontal resolution sensitivity in a climate model. *Climate Dyn.,* **19,** 211–216.

Ringer, M. A., and Coauthors, 2006: The physical properties of the atmosphere in the new Hadley Centre Global Environmental Model (HadGEM1). Part II: Aspects of variability and regional climate. *J. Climate,* **19,** 1302–1326.

Sardeshmukh, P. D., and B. J. Hoskins, 1988: The generation of global rotational flow by steady idealized tropical divergence. *J. Atmos. Sci.,* **45,** 1228–1251.

Stephenson, D. B., V. Pavan, M. Collins, M. M. Junge, and R. Quadrelli, 2006: North Atlantic Oscillation response to transient greenhouse gas forcing and the impact on European winter climate: A CMIP2 multi-model assessment. *Climate Dyn.,* **27,** 401–420.

Stratton, R. A., 2004: Report on aspects of variability in high-resolution versions of HadAM3. Met Office Hadley Centre Tech. Note 53, 32 pp.

Uppala, S. M., and Coauthors, 2005: The ERA-40 Re-Analysis. *Quart. J. Roy. Meteor. Soc.,* **131,** 2961–3012.

Vellinga, M., and R. A. Wood, 2002: Global climatic impacts of a collapse of the Atlantic thermohaline circulation. *Climatic Change,* **54,** 251–267.

——, and P. Wu, 2008: Relations between northward ocean and atmospheric energy transports in a coupled climate model. *J. Climate,* **21,** 561–575.

——, ——, and J. M. Gregory, 2002: Processes governing the recovery of a perturbed thermohaline circulation in HadCM3. *J. Climate,* **15,** 764–780.

Wilks, D. S., 1995: *Statistical Methods in the Atmospheric Sciences*. Academic Press, 648 pp.

Zhang, R., and T. L. Delworth, 2005: Simulated tropical response to a substantial weakening of the Atlantic thermohaline circulation. *J. Climate,* **18,** 1853–1860.